Coupling of Sequential Transitions in a DNA Double Hairpin: Energetics, Ion Binding, and Hydration[†]

Dionisios Rentzeperis, Dmitrii P. Kharakoz,[‡] and Luis A. Marky*

Department of Chemistry, New York University, New York, New York 10003
Received January 22, 1991; Revised Manuscript Received March 29, 1991

ABSTRACT: In an effort to evaluate the relative contributions of sequence, ion binding, and hydration to the thermodynamic stability of nucleic acids, we have investigated the melting behavior of a double hairpin and that of its component single hairpins. Temperature-dependent UV absorption and differential scanning calorimetry techniques have been used to characterize the helix–coil transitions of three deoxyoligonucleotides: d(GTACT$_5$GTAC), d(GCGCT$_5$GCGC), and d(GCGCT$_5$GCGCGTACT$_5$GTAC). The first two oligomers melt with transition temperatures equal to 28 and 69 °C, respectively, in 10 mM dibasic sodium phosphate at pH 7.0. The T_m's are independent of strand concentration, strongly indicating the presence of single-stranded hairpin structures at low temperatures. The third oligomer, with a sequence corresponding to the joined sequences of the first two oligomers, melts with two apparently independent monomolecular transitions with T_m's of 41 and 69 °C. These transitions correspond to the melting of a double hairpin. In the salt range of 10–100 mM in NaCl, we obtain average enthalpies of 24 and 38 kcal/mol for the transitions in the single-hairpin molecules. Each transition in the double hairpin has an enthalpy of 32 kcal/mol. In addition, $dt_m/d \log [\text{Na}^+]$ for the transitions are 4.1 and 4.7 °C for the single hairpins and 12.6 and 11.2 °C for each transition in the double hairpin. The differential ion binding parameter between the double hairpin and that of the sum of single hairpins is roughly equal to 1.1 mol of Na$^+$ ions/mol of double hairpin and is consistent with an increase in the electrostatic behavior of the stem phosphates of this molecule. Thermodynamic profiles at 5 °C reveal that each thermodynamic parameter ($\Delta G°$, $\Delta H°$, and $\Delta S°$) for the formation of the double hairpin is equal to the sum of the thermodynamic parameters of the two single hairpins. Combined measurements of ultrasound velocities and densities at 5 °C allows us to determine the apparent molar volume and the apparent molar adiabatic compressibility of each molecule. The values for the double hairpin correspond roughly to the sum of the individual contributions of the single-hairpin molecules and agree with the additivity of our CD spectra. A close inspection of the parameters for the transitions in the double hairpin relative to the corresponding transitions in the single hairpins indicates that the stabilization of the first transition is accompanied by a more favorable enthalpy together with an increase in the amount of bound sodium ions, while the second transition is accompanied by a more favorable entropy. The apparent molar volume and apparent molar adiabatic compressibility values for each single hairpin indicate that the hairpin with the GTAC/CATG stem is more hydrated than the hairpin with GCGC/CGCG stem.

Ⅰn the past decade, there have been intensive investigations of the formation and physical properties of hairpin structures in synthetic DNA fragments with particular emphasis on establishing the structure of these molecules (Haasnoot et al., 1980, 1983, 1986; Hare & Reid, 1986; Ikuta et al., 1986; Summers et al., 1985; Wemmer et al., 1985; Chattopadhyaya et al., 1988; Williamson & Boxer, 1989a,b; Wolk et al., 1988), the overall thermodynamics of hairpin formation (Paner et al., 1990), and the effects of sequence and loop size on the stability of hairpins (Amaratunga et al., 1989; Benight et al., 1989; Erie et al., 1987; Hilbers et al., 1985; Senior et al., 1988; Wemmer & Benight, 1985; Xodo et al., 1986, 1988a,b). Hairpin structures are common in RNA molecules (Erdmann, 1980). The formation of looped out structures in DNA has been postulated to exist in DNA regions with palindromic sequences. These sequences have been implicated as regions involved in gene regulation (Maniatis et al., 1975; Muller & Fitch, 1982;

Rosenberg & Court, 1979; Wells et al., 1980). Supercoiling of DNA generates looped out cruciform structures (Courey & Wang, 1988; Frank-Kamenetskii & Vologodskii, 1984; Lilley, 1980, 1981; Panayotatos & Wells, 1981). Short self-complementray DNA oligonucleotides with proper sequences also form hairpin structures at low salt and low strand concentrations (Marky et al., 1983; Patel et al., 1983; Wemmer et al., 1985).

Oligonucleotides of defined sequence are useful models for the structural features found in naturally occurring nucleic acid polymers. Thermodynamic investigations of the helix–coil transition of these oligomer molecules have greatly enhanced our understanding of the structures and conformational transitions of DNA and RNA molecules (Albergo et al., 1981; Gralla & Crothers, 1973; Marky et al., 1981; Uhlenbeck et al., 1973). These studies have provided the basis for the thermodynamic characterization of the molecular forces that control the structure and conformation of nucleic acids (Breslauer et al., 1986; Freier et al., 1986). Short single-stranded hairpin DNA molecules are favorable for such thermodynamic studies because they form stable intramolecular duplexes. Their thermodynamic characterization is greatly simplified because transitions tend to be monomolecular

and take place at convenient experimental temperatures.

We are most interested in understanding the contributions of hairpin loops to the stability of nucleic acids and the effect of sequence in the melting behavior of nucleic acids. We are currently investigating the effect of temperature and hydration on the helix–coil transition of short DNA hairpins with at least four base pairs in the stem. We present here a full thermodynamic description of the melting behavior of the structures formed by the sequences d(GTACT$_5$GTAC), d-(GCGCT$_5$GCGC), and the combined sequence d-(GCGCT$_5$GCGCGTACT$_5$GTAC). Our experimental results demonstrate that these oligonucleotides form stable single-stranded hairpins. We were able to evaluate the overall energetics, conformational flexibility hydration, and ion binding that accompanies the formation of a double hairpin from two single hairpins by comparing the melting of the two independent short DNA domains with the melting of the same domains when combined.

MATERIALS AND METHODS

Materials. The oligomers, d(GCGCT$_5$GCGC), d-(GTACT$_5$GTAC), and d(GCGCT$_5$GCGCGTACT$_5$GTAC), were synthesized on an ABI 380B automated synthesizer, with use of standard phosphoramidite chemistry, purified by HPLC, and desalted on a Sehadex G-10 exclusion chromatography column. Extinction coefficients of the oligomers in single strands were calculated at 25 °C by use of the tabulated values of the dimers and monomer bases (Cantor et al., 1970) and estimated at high temperatures by extrapolation to 25 °C of the upper portions of the melting curves (Marky et al., 1981), which corresponds to the UV–temperature dependence of the single strands. The concentrations of the oligomers were determined in water with use of the following extinction coefficients in single strands at high temperatures: $\epsilon_{260,70°C}$ = 1.21 × 10^5 M^{-1} cm^{-1} for d(GTACT$_5$GTAC); $\epsilon_{260,90°C}$ = 1.08 × 10^5 M^{-1} cm^{-1} for d(GCGCT$_5$GCGC); and $\epsilon_{260,90°C}$ = 2.32 × 10^5 M^{-1} cm^{-1} for d(GCGCT$_5$GCGCGTACT$_5$GTAC). All other chemicals were reagent grade. The buffer solutions consisted of 10 mM NaP$_i$,[1] pH 7.0, and 0.1 mM EDTA, adjusted to the desired ionic strength with NaCl. Stock oligomer solutions were prepared by directly dissolving dry and desalted oligomers in the appropriate buffer.

UV Melting Curves. Absorbance versus temperature profiles (melting curves) in appropriate solution conditions at strand concentrations of 3–65 μM were measured at 260 or 275 nm depending on the hyperchromicity of the melted base pairs of a given transition. For comparison with the calorimetric curves, melting curves were also performed at 268 nm with a strand concentration of 60 μM. At this wavelength we monitor a measurable hyperchromicity for both AT and GC base pairs. These melting curves were obtained with a thermoelectrically controlled Perkin-Elmer 552 spectrophotometer interfaced to a PC-XT computer for acquisition and analysis of experimental data. The temperature was scanned at a heating rate of 1.0 °C/min. These melting curves allow us to measure the transition temperatures, T_m, and van't Hoff enthalpies, ΔH_{vH}. These parameters were calculated according to standard procedures reported elsewhere and correspond to a two-state approximation of the helix-coil transition of each molecule (Marky et al., 1981; Marky & Breslauer, 1987). $\Delta A/\Delta t$ vs temperature curves were obtained by directly taking

absorbance differences at 1-degree intervals of the experimental curves.

Salt Dependence of Transition Temperatures. UV melting curves were also carried out in the same buffer at a similar strand concentration of 5 μM in the range of 0–100 mM NaCl. The purpose of these experiments is to obtain the slopes of T_m vs log [Na$^+$] plots, which are proportional to the thermodynamic release of couterions per mole of DNA duplex, Δn, in the helix–coil transition of DNA oligomers. The relevant equation is

$$\mathrm{d}T_m/\mathrm{d}\log[\mathrm{Na}^+] = -0.9(2.303RT_m^2/\Delta H°)\Delta n$$

The negative sign is to indicate a release of counterions; the value of 0.9 is a correction factor that corresponds to the conversion of mean ionic activities to concentrations; the term in parenthesis includes R, which is the gas constant in calories per Kelvin per mole, and $\Delta H°$ (in calories per mole of duplex), the standard dissociaton enthalpy, which is measured directly with differential scanning calorimetry (Record et al., 1978; Manning, 1978). The counterion release obtained in this way corresponds to the stoichiometric ion release of the melting of one cooperative unit; in two-state transitions this cooperative unit is equal to the dissociaton of the entire duplex. The Δn values in moles of sodium ions released per duplex can be normalized per phosphate by taking into account the number of phosphates that are involved in a given transition (stem and loop) or the number of phosphates in the stem of these molecules.

Circular Dichroism (CD) Spectroscopy. Spectra were recorded on an AVIV 60DS spectrometer (Aviv Associates, Lakewood, NJ). The temperature of the cell was kept at 5 °C with use of a Hewlett-Packard 891000-A temperature controller. Spectra of solutions with an optical density ranging from 0.7 to 0.8 at 260 nm were obtained at 220–320 nm every 1 nm with 0.1-cm cells. Final spectra represent the average of at least three scans.

Differential Scanning Calorimetry (DSC). Excess heat capacity as a function of temperature for each oligomer was measured with a Microcal MC-2 differential scanning calorimeter. Typically an oligomer solution with a concentration in the range of 0.7–1.1 mM (in strands) dissolved in buffer was scanned against the same buffer from 5 to 100 °C at a heating rate of 45 °C/h. For the analysis of the experimental data, a buffer versus buffer scan is subtracted from the sample vs buffer scan; both scans in the form of millicalories per second vs temperature were converted to millicalories per degree Celsius vs temperature by dividing each experimental data point by the corresponding heating rate. The area under the resulting curve is proportional to the total heat of the transition and when normalized for the number of millimoles is equal to the transition enthalpy, ΔH_{cal}. The instrument was calibrated with a standard electrical pulse. Shape analysis of the heat capacity curves is included in the software of the instrument and allows us to calculate two-state enthalpies, ΔH_{vH}. Direct comparisons of ΔH_{vH} with ΔH_{cal} enable us to predict the nature of the transition. For the sequential transitions of the double hairpin, enthalpies were obtained by deconvolution of the experimental curves, with use of the software supplied with the instrument by Microcal, Inc. (Northampton, MA). In this deconvolution it was assumed that the two transitions were independent and each transition had a $\Delta C_p = 0$.

Density Measurements. An Anton Paar DMA 60 densitometer equipped with two DMA 602 microcells was used for the differential measurement of the density of solutions of each molecule at appropriate temperatures in low salt buffer. The

---

[1] Abbreviations: CD, circular dichroism; DSC, differential scanning calorimetry; NaP$_i$, dibasic sodium phosphate; EDTA, ethylenediaminetetraacetic acid.

Table I: Spectroscopic and Calorimetric Melting Results[a]

hairpin	UV		calorimetry		
	t_m (°C)	ΔH_{vH} (kcal/mol)	t_m (°C)	ΔH_{vH} (kcal/mol)	ΔH_{cal} (kcal/mol)
G-T-A-C ⌐ T5 / C-A-T-G ⌐	28.3	24	28.3	23	23.2
	(33.4)	(26)	(32.8)	(25)	(23.9)
G-C-G-C ⌐ T5 / C-G-C-G ⌐	71.0	38	69.2	38	39.2
	(75.7)	(39)	(73.9)	(39)	(37.2)
	40.4	32	40.5	32	31.3
T5 G-T-A-C G-C-G-C T5 / C-A-T-G-C-G-C-G	(50.1)	(29)	(48.2)	(31)	(33.5)
	68.6	42	69.0	40	33.2
	(76.1)	(44)	(75.1)	(42)	(31.0)

[a] Values were taken in 10 mM sodium phosphate buffer and 0.1 mM Na₂EDTA at pH 7.0 (0.1 M NaCl is included for values in parentheses). Transition temperatures were within ±0.5 °C, ΔH_{vH} were within ±7% of absolute values, and ΔH_{cal} were within ±3% of absolute values. The first set of data of the double hairpin corresponds to the melting of the GTAC/CATG stem.

instrument was calibrated with the known densities of air and water. The temperature of the cell was kept at 5 ± 0.001 °C with a Forma bath and a Tronac temperature controller. Apparent molar volumes, Φ_V, have been calculated from the densities by standard procedures (Hoiland, 1986).

Ultrasound Velocity Measurements. A differential acoustic resonator developed in the Institute of Biological Physics of the USSR Academy of Sciences (Sarvazyan & Kharakoz, 1981; Shestimirov & Sarvazyan, 1986) was used to measure ultrasound velocities of the oligomer solutions. The stainless steel acoustic cells have a sample volume of 0.8 mL; all solutions have a concentration of about 1 mM in strands. The relative accuracy of each measurement is estimated to be 2 × 10⁻⁴%. The temperature of both cells was kept at 5 ± 0.001 °C. The technique and the calculation of the apparent molar compressibility, Φ_{ks}, from ultrasonic and densitometric data have been described elsewhere (Buckin, 1989a,b). This parameter can be used to estimate the hydration of DNA molecules in solution.

RESULTS

UV Melting Curves. The helix–coil transition of the ordered structures formed by the deoxyoligonucleotides d-(GTACT₅GTAC), d(GCGCT₅GCGC), and d-(GCGCT₅GCGCGTACT₅GCAC) in appropriate buffer conditions was characterized by UV melting curves. Typical ΔA versus Δt profiles are shown in Figure 1. The transition temperatures and the corresponding van't Hoff enthalpies for all three oligomers at two different salt concentrations are listed in Table I. The melting of d(GTACT₅GTAC) (hairpin 1) and d(GCGCT₅GCGC) (hairpin 2) occurs in standard monophasic transitions; however, d(GCGCT₅GCGCGTACT₅GTAC) (double hairpin) melts in a biphasic transition, with a T_m for the first transition of 12 °C higher than the T_m of d(GTACT₅GTAC) and a T_m for the second transition of 0.2 °C lower than the T_m of d(GCGCT₅GCGC). In all cases the transitions are very broad, covering a temperature range of about 40 °C with van't Hoff transition enthalpies characteristic of the sum of the nearest-neighbor stacking interactions present in each molecule. In these optical melts, an increase in the oligomer concentration from 3 to 65 μM has no effect on the T_m of each transition in these three molecules. This T_m independence from the concentration of oligomer, together with the high observed T_m values and transition enthalpies, is
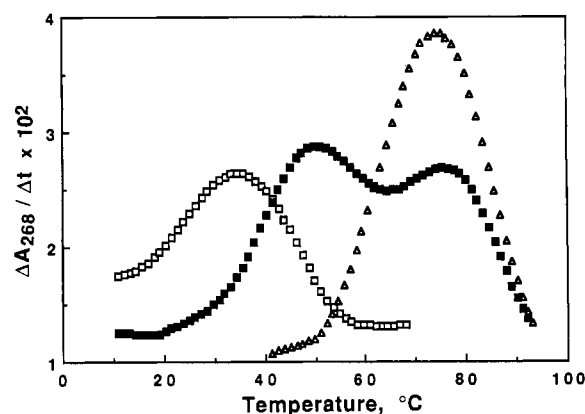

FIGURE 1: Typical $\Delta A/\Delta t$ profiles recorded at 268 nm for d-(GTACTTTTTGTAC) (□), d(GCGCTTTTTGCGC) (△), and d-(GCGCTTTTTGCGCGTACTTTTTGTAC) (■), in 10 mM NaPᵢ buffer/0.1 mM Na₂EDTA/0.1 M NaCl at pH 7. All oligomer solutions have a concentration of 60 μM in strands. Similar profiles were obtained with oligomer concentrations as low as 3 μM.
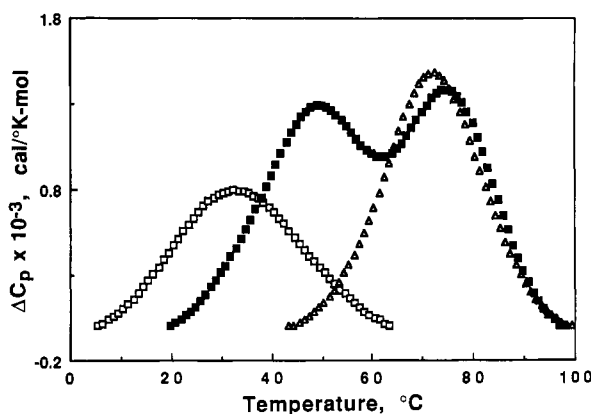

FIGURE 2: Typical excess molar heat capacity curves relative to buffer for d(GTACTTTTTGTAC) (□), d(GCGCTTTTTGCGC) (△), and d(GGCCTTTTTGCGCGTACTTTTTGTAC) (■), in 10 mM NaPᵢ buffer/0.1 mM Na₂EDTA/100 mM NaCl at pH 7. All oligomer solutions have a concentration of 0.800 mM in strands.

consistent with the unimolecular melting of single-stranded hairpins.

Calorimetry and Nature of the Transitions. Typical excess heat capacity versus temperature profiles (Figure 2) present
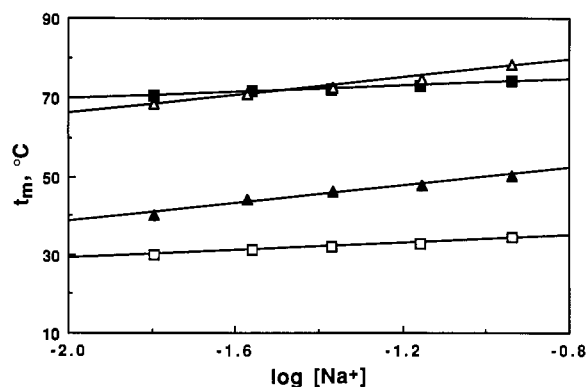
FIGURE 3: t_m vs log [Na$^+$] plots of d(GTACTTTTTGTAC) (□), d(GCGCTTTTTGCGC) (■), d(GCGCTTTTTGCGCGTACT-TTTTGTAC): first transition (▲) and second transition (△), in 10 mM NaP$_i$ buffer/0.1 mM Na$_2$EDTA at pH 7.

features similar to the UV melting curves. The area under these curves is proportional to the total heat needed to disrupt these duplexes into single strands. These heats when normalized for the total number of moles of strands are equal to the molar enthalpies. Transition temperatures and the corresponding van't Hoff and calorimetric enthalpies measured from these curves are listed in Table I. Relative to the UV melts, we obtained similar transition temperatures despite the 100-fold increase in concentrations. The transition enthalpies of the single hairpins are characteristic of the sum of the nearest-neighbor stacking interactions present in these molecules. In the case of the double hairpin relative to the single hairpins, we measured an increase of 8.8 kcal/mol in the enthalpy values for the first transition and a decrease of 6.1 kcal/mol for the second transition. This gives a net enthalpy change of 2.7 due to the extra base-pair stack. Comparison of the van't Hoff enthalpies, calculated from the shape of the calorimetric or spectroscopy curves (Marky & Breslauer, 1987), with the transition enthalpies, measured directly by differential scanning calorimetry, allows us to draw conclusions about the nature of these transitions. In this range of salt concentration, we obtained a $\Delta H_{vH}/\Delta H_{cal}$ ratio of 1.04 and 1.00 for each of the single hairpins and 0.97 and 1.34 for the transitions in the double hairpin. All four transitions melt in a two-state transition manner. However, the second transition (GCGC/CGCG) of the double hairpin has an unusual $\Delta H_{vH}/\Delta H_{cal}$ ratio that could be due to a high estimation of the van't Hoff enthalpy in the deconvolution analysis. This unusual ratio has been observed previously with oligomers containing frayed ends (Marky et al., 1981).

Ionic Strength Dependence. Figure 3 contains plots of the transition temperature versus log [Na$^+$]. Table II lists the slopes of such plots as well as the values of the constants used to calculate the counterion release parameters for each transition. The value of $RT_m^2/\Delta H_{cal}$ was obtained directly from the calorimetric curves and corresponds to the average of five scans each at 0 and 0.1 M NaCl in the same phosphate buffer. For the melting transitons of the single hairpins, we obtained values of 4.1 and 4.7 °C for the slopes of such plots. This weak dependence on the salt concentration is characteristic of ion release processes that take place with DNA hairpin duplexes with four base pairs (Marky et al., 1983; and unpublished results), providing further evidence for the exclusive formation at low temperatures of short hairpin structures. On the other hand, for the transitions of the double hairpin, the resulting slopes are equal to 12.6 and 11.2 °C, which are characteristic of the melting of duplexes containing eight base pairs (Zolandz, 1986; Erie et al., 1987; unpublished results). In terms of Δn,

Table II: Parameters Used to Calculate Counterion Release[a]

hairpin	$dT_m/$ d log [Na$^+$] (°K)	$RT_m^2/\Delta H_{cal}$ (°K/mol)	Δn (mol of Na$^+$/ mol of duplex)
G-T-A-C • • • • T_5 C-A-T-G	4.1	7.78	0.254
G-C-G-C • • • • T_5 C-G-C-G	4.7	6.19	0.366
G-T-A-C G-C-G-C T_5 • • • • • • • • T_5 C-A-T-G-C-G-C-G	12.6	6.19	0.982
	11.2	7.39	0.731

[a]The slopes of the T_m vs log [Na$^+$] plots were obtained by least-squares analysis with at least 99% confidence level. The values of $RT_m^2/\Delta H_{cal}$ represent the average of at least five determinations each in both low and high salt buffer solutions, with an absolute error of ±3.5%. The values of Δn are ±5.0%. The first set of data of the double hairpin corresponds to the melting of the GTAC/CATG stem.
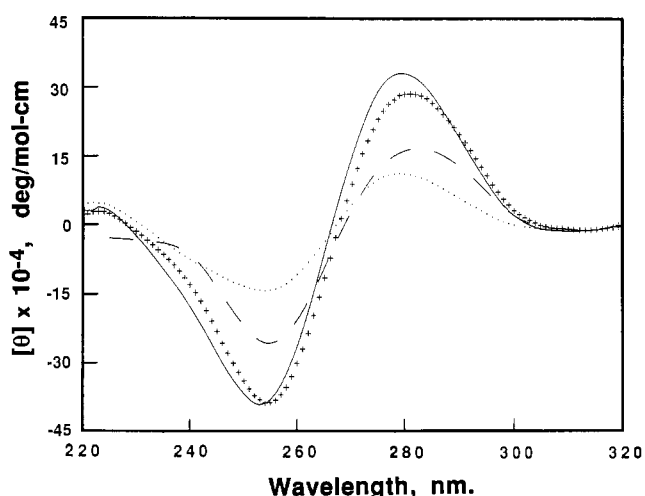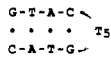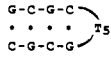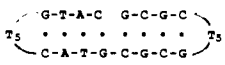

FIGURE 4: CD spectra of hairpins in 10 mM NaP$_i$ buffer/0.1 mM EDTA at pH 7 and 5 °C: d-(GCGCTTTTTGCGCGTACTTTTTGTAC) (—), d-(GTACTTTTTGTAC) (···), d(GCGCTTTTTGCGC) (−−), and the additive spectra of single hairpins (+ +).

we measured a thermodynamic ion release of 0.25 (hairpin 1) and 0.37 (hairpin 2) sodium ions/mol of hairpin for each of the single hairpins; for the double hairpin these values are respectively 0.98 and 0.73 for each transition. In terms of the electrostatic ion release, the disruption of each single hairpin versus the disruption of the equivalent sequence in the double hairpin, each transition has an apparent increase of ionic co-operativity from four to eight base pairs. The higher Δn value obtained for the first transition relative to the second transition of the double hairpin indicates that the extra phosphate in the double hairpin is included in the melting of the GTAC/CTAG stem of the double hairpin.

Circular Dichroism. Figure 4 shows the CD spectra for all three molecules at 5 °C, a temperature at which all three molecules are forming fully helical structures. The shape of each spectrum is characteristic of a B-DNA. The spectrum of the double hairpin is qualitatively equal to the sum of the spectra of each single hairpin, indicating that base-stacking interactions and sugar—phosphate backbone conformations that are present in each single-hairpin molecule are nearly identical with the ones present in the double hairpin.

Partial Molar Volumes and Adiabatic Compressibilities. The results of our density and ultrasound velocity measurements at 5 °C are listed in Table III. At this temperature

Table III: Ultrasound Velocities and Adiabatic Compressibilities at 5 °C[a]

hairpin	[u] (cm/s)	ϕ_v (cm³/ mol)	$\phi_{ks} \times 10^4$ (cm³/mol· bar)
G-T-A-C ⌐ • • • • T5 C-A-T-G ⌐	1442	1875	-1880
G-C-G-C ⌐ • • • • T5 C-G-C-G ⌐	1359	1985	-1786
⌐ G-T-A-C G-C-G-C ⌐ T5 • • • • • • • • T5 ⌐ C-A-T-G-C-G-C-G ⌐	2841	3478	-3846

[a]Values were taken in 10 mM sodium phosphate buffer and 0.1 mM Na₂EDTA at pH 7.0. The values of ϕ_v are within ±2.7% and of ϕ_{ks} are within ±3.5%.

all three molecules are single-stranded hairpins with sodium ions in their hydration shells. The values of the apparent molar volume, ϕ_v, and apparent adiabatic compressibility, ϕ_{ks}, provide qualitative information on the hydration state of each molecule (Buckin, 1989a,b). The values of ϕ_v and ϕ_{ks} for hairpin 1 are lower than those for hairpin 2. Therefore, hairpin 1 is slightly more hydrated than hairpin 2. In addition, the sum of these values is roughly equal to the values of the double hairpin. This last result indicates that the overall hydration of the double hairpin is identical with the sum of the hydration of the individual hairpins.
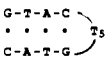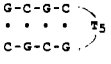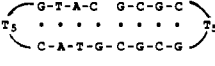
Thermodynamic Profiles at Low Temperatures. In order to directly compare the thermodynamic parameters for these molecules (Table IV), $\Delta G°$ and $T\Delta S°$ were calculated at 5 °C, a temperature at which the stems in each hairpin are fully ordered. The $\Delta G°$ at 5 °C for each molecule was determined as follows: For the monomolecular unfolding of a single-stranded hairpin, at T equal to the T_m, $K = 1$, $\Delta G° = 0$, and $\Delta S° = \Delta H°/T_m$. Substitution of this last expression into the Gibbs equation, and assuming the enthalpy to be independent of temperature ($\Delta C_p = 0$), we obtain $\Delta G_T = \Delta H(1 - T/T_m)$.

DISCUSSION

Overall Free Energy of Formation. Each deoxyoligonucleotide used in this study can adopt in principle helical complexes in solution that involve one to several strands. The particular complex or predominant structure in solution will depend on its overall free energy of formation, ΔG_f, which is equal to the sum of the nucleation free energy, ΔG_{nuc}, propagation free energy, ΔG_{prop}, and loop free energy, ΔG_{loop}. It is reasonable to assume that the nucleation as well as the loop free energy terms for all three molecules are similar; all molecules have five thymines in the loop. Therefore, any differences in the overall free energy of formation can be attributed to differences in the sequences of the helical stem. Experimentally, ΔG_f depends on the oligomer sequence, loop sequence, loop length, salt concentration, oligomer concentration, degree of hydration, and temperature. In the following sections, we discuss the exclusive formation of intramolecular hairpin duplexes and the thermodynamic behavior of the helix–coil transition of each single hairpin as well as the sequential melting of the transitions in the double hairpin. We emphasize the thermodynamic and ionic behavior of creating an extra base-pair stack in the double hairpin as the result of joining the two single hairpins.

Experimental Evidence for Monomolecular Transitions. Comparison of the UV melting profiles at a 60 μM strand

Table IV: Thermodynamic Profiles for the Formation of Hairpins at 5 °C[a]

hairpin	$\Delta G°$ (kcal/mol)	$\Delta H°$ (kcal/mol)	$T\Delta S°$ (kcal/mol)
G-T-A-C ⌐ • • • • T5 C-A-T-G ⌐	-1.8 (-2.2)	-23.2 (-23.9)	-21.4 (-21.7)
G-C-G-C ⌐ • • • • T5 C-G-C-G ⌐	-7.4 (-7.4)	-39.2 (-37.2)	-31.8 (-29.8)
Sum of two hairpins	-9.2 (-9.6)	-62.4 (-61.1)	-53.2 (-51.5)
⌐ G-T-A-C G-C-G-C ⌐ T5 • • • • • • • • T5 ⌐ C-A-T-G-C-G-C-G ⌐	-3.5 (-4.5) -6.2 (-6.2)	-31.3 (-33.5) -33.2 (-31.0)	-27.8 (-29.0) -27.0 (-24.8)
Sum of two transitions	-9.7 (-10.7)	-64.5 (-64.5)	-54.8 (-53.8)

[a]Values were taken in 10 mM sodium phosphate buffer and 0.1 mM Na₂EDTA at pH 7.0 (0.1 M NaCl is included for values in parentheses).

concentration with the calorimetric curves performed at 800 μM (see Figures 1 and 2) indicates that the transition temperatures for all three molecules are independent of oligomer concentration. In addition, at the range of ionic strengths used in melting experiments, the magnitudes of these T_m's (28.3 and 69.2 °C for the single hairpins) are much higher than the T_m's (<0 and 22 °C, in 1 M NaCl) predicted from the stem sequence for the melting of the intermolecular duplexes with internal loops, assuming an internal loop free energy contribution of zero to the overall free energy of duplexation (Breslauer et al., 1986; Marky et al., 1987). These results provide strong evidence that only unimolecular complexes are formed in solution. Furthermore, the transition enthalpies (23 and 39 kcal/mol) and the salt dependence of the transition temperature ($\sim$4.5 °C) for the single hairpins are consistent with the four base pairs that constitute the short helical stem of these hairpin molecules. The overall transition enthalpy of the double hairpin is 64.5 kcal/mol and is consistent with a stem of eight base pairs. These results provide strong circumstantial evidence of the formation of intramolecular partial duplexes for all three molecules.

A further indication for the formation of intramolecular hairpins in our system is the observed thermal stabilization of 41 °C of hairpin 2 relative to hairpin 1 over the range of salt concentrations in our studies. This differential stabilization corresponds to a more favorable stacking free energy of about 6.3 kcal/mol due to the substitution of one each of the GT/CA, TA/AT, and AC/TG base-pair stacks by two GC/CG and one CG/GC stacks (Breslauer et al., 1986). This stabilization is 16 °C higher than the 25 °C difference in T_m's between the hairpins formed by the sequences d-(CGAACGT₄CGTTCG) (Senior et al., 1988) and d-(CGCGCGT₄CGCGCG) (Ikuta et al., 1986) at similar salt concentrations. In this pair of hairpin molecules, the base-pair stacks GA/CT, AA/TT, and AC/TG are replaced by two GC/CG and one CG/GC stacks to give a more favorable free energy of 5.0 kcal/mol. Thus, our two hairpins have 1.3 kcal/mol more favorable free energy, which corresponds to

an extra differential stabilization of 7 °C. The overall discrepancy of 9 °C could be due to differences in the size of the loop (four thymines versus five in our oligomers), differences in the values of the nearest-neighbor stacking free energies (obtained in 1 M NaCl), and the different bases at the 5′ end (C vs G).

Thermodynamic Coupling of Transitions. In this range of salt concentrations, comparison of the T_m's of the transitions observed in the double hairpin with the corresponding transition of each single hairpin reveals that the T_m of the first transition of the double hairpin, melting of the GTAC/CATG stem, occurs with a T_m stabilization relative to the single hairpins of 12.2–15.2 °C, while the second transition of the double hairpin, melting of GCGC/CGCG stem, is stabilized only –0.2–1.2 °C. These results can be explained in terms of the presence of an extra C-G/G-C base stack at the gap of the double hairpin. The sum of the free energies of formation of both transitions in the double hairpin is equal to the sum of the free energies of formation of the single hairpins, but the free energy of each transition within the double hairpin is different from the corresponding transition in the single hairpin. Specifically, in this range of salt concentrations, we measured a more favorable ΔG_f of about 1.5 kcal/mol on the average for the first transition and 1.2 kcal/mol less favorable ΔG_f for the second transition.

Dissection of these free energies into their enthalpic and entropic contributions reveals that the sum of the enthalpies of both transitions in the double hairpin is also equal to the sum of the enthalpies of the single hairpins. However, close inspection of the enthalpies of these transitions indicates that the stabilization of the first is enthalpic, as seen with a more favorable enthalpy of 8.9 kcal/mol and an unfavorable entropic term of 6.9 kcal/mol. These parameters correspond to the formation of an extra base-pair stack at the gap of the double hairpin. The small stabilization of the second transition is accompanied by a less favorable enthalpy of 6.1 kcal/mol and a more favorable entropy of 4.9 kcal/mol, suggesting an enthalpy–entropy coupling that takes place within the transitions of the double hairpin. The observed additivity in the overall ΔG_f at 5 °C is in good agreement with the additivity of our circular dichroism spectra and apparent molar adiabatic compressibility values.

Thermodynamic Counterion Release. Our salt-dependence measurements estimate the thermodynamic counterion release of these transitions. In order to compare our values with similar studies of oligomeric systems, we have estimated the counterion release per phosphate, Δi. We divide our Δn values by the total number of phosphates that are involved in each transition: 12 phosphates for the single hairpins and for the second transition of double hairpin (6 in the stem and 6 in the loop) and 13 for the first transition of double hairpin. We obtained a $\Delta i = 0.021$ and 0.031 for the single hairpins; these values are in good agreement with the estimated value of 0.027 for the hairpin formed by the sequence d-(CGCGAATTCGCG) (Marky et al., 1983; unpublished results). For the transitions of the double hairpin, we obtained Δi's of 0.075 and 0.061. These values are in fair agreement with the Δi range of 0.086–0.131 obtained with octameric duplexes containing 14 phosphates and different base sequences (Zolandz, 1985; Erie et al., 1987). Alternatively, if the loop phosphates behave electrostatically as single-stranded phosphates, we obtained Δi values of 0.140 and 0.122, which are close to the value of $\Delta i = 0.17$ for the melting of DNA polymers. The results of our calorimetric measurements indicate similar enthalpic values for the sum of single hairpins

and that of the overall enthalpy of the double hairpin, ruling out the possibility that the bases in the loops are stacked and that the loop phosphates behave electrostatically as helical phosphates. It is obvious that structural information is needed to completely distinguish between these two possibilities.

The net effect is that the formation of the double hairpin from two single hairpins is accompanied by an increase in the amount of bound counterions equal to 1.09 mol of sodium ions/mol of duplex. Since we have five thymines in the loops, the optimum number for the stability of a DNA hairpin, these residues have the flexibility to behave like partial random coils. An explanation for this differential counterion binding is that in the initial helical states of these molecules the GC base pairs at the ends of the single hairpins are more exposed to solvent than the same GC that are forming CG/G-C base-pair stack (with a nick) at the center of the double hairpin. Thus, the whole stem of the double hairpin behaves electrostatically as a helical section of a DNA polymer.

Hydration Effects. To examine the hydration of these molecules, acoustical and density measurements were carried out at 5 °C. These results indicate that the GTAC hairpin is somewhat more hydrated than the GCGC hairpin. The difference in the adiabatic compressibilities of the single hairpins corresponds to a rough estimation of 5–10 water molecules in the differential number of bound water (Buckin et al., 1989a; Marky & Kupke, 1989). This is expected for sequences with a higher percentage of AT base pairs (Buckin et al., 1989a). The sum of the molar specific volumes and molar adiabatic compressibilities of these molecules plus the contribution of the extra phosphate (at the gap), equal to –170 × 10^{-4} cm³/mol·bar (Conway, 1981), is approximately the same as that of the double hairpin, within experimental error. This means that the overall combined amount of bound water molecules and bound counterions in the double hairpin is approximately the same as the sum of the two single hairpins and indicates perhaps a change in the nature of the bound water.

CONCLUSIONS

We have characterized thermodynamically the helix–coil transition of two single hairpins with different base sequences and that of the combined sequence that forms a double hairpin. Our standard thermodynamic parameters and ϕ_{ks} values for all three molecules indicate that the overall energetics of the double hairpin is close to the sum of the energies of the single hairpins. This implies that there is no structural perturbation in joining the individual hairpins to create the double hairpin. However, the energies observed in the transition of the double hairpin relative to the corresponding single hairpins are perturbed, as detected by shifts in the T_m and ionic interaction parameters (Figures 1 and 2). One obvious reason for the differences is the presence of the extra base-pair stack that forms at the gap of the double hairpin. A second is that the range of electrostatic interactions at low salt concentrations is long enough to cause an interaction between the two transitions. This represents an example of linkage in nucleic acid transitions that is salt dependent; at high salt this coupling would be expected to disappear. This situation is parallel to that in tRNA (Privalov & Filimonov, 1978).

The perspective of these studies is that if one is to fully understand the melting behavior of natural nucleic acids, one needs to take into account the effect of ions and water molecules on the stabilization of nucleic acids. It is obvious that more sequences are needed to build a consistent set of these interactions. However, this type of approach of building a complex DNA molecule from the combination of short melting

domains may be useful in predicting the sequential melting of domains that occur in DNA plasmids.

REFERENCES

Albergo, D. D., Marky, L. A., Breslauer, K. J., & Turner, D. H. (1981) *Biochemistry 20*, 1409–1413.

Amaratunga, M., Pancoska, P., Paner, T. M., & Benight, A. S. (1989) *Nucleic Acids Res. 18*, 577–582.

Benight, A. S., Wang, Y. W., Amaratunga, M., Chattopadhyaya, R., Henderson, J., Hanlon, S., & Ikuta, S. (1989) *Biochemistry 28*, 3323–3332.

Breslauer, K. J., Frank, R., Blocker, H., & Marky, L. A. (1986) *Proc. Natl. Acad. Sci. U.S.A. 83*, 3746–3750.

Buckin, V. A., Kankiya, B. I., Burlichov, N. V., Lebedev, A. V., Gukovsky, I. Ya., Chuprina, V. P., Sarvazyian, A. P., & Williams, A. R. (1989a) *Nature (London) 340*, 321–322.

Buckin, V. A., Kankiya, B. I., Sarvazyian, A. P., & Uedaira, H. (1989b) *Nucleic Acids Res. 17*, 4189–4203.

Cantor, C. R., Warshow, M. M., & Shapiro, H. (1970) *Biopolymers 9*, 1059–1077.

Chattopadhyaya, R., Ikuta, S., Grzewskowiak, K., & Dickerson, R. E. (1988) *Nature (London) 334*, 175–179.

Conway, B. E. (1981) in *Ionic Hydration in Chemistry*, Elsevier, Amsterdam.

Courey, A. J., & Wang, J. C. (1988) *J. Mol. Biol. 202*, 35–43.

Erdmann, V. A. (1980) *Nucleic Acids Res. 8*, r31–r47.

Erie, D., Sinha, N., Olson, W., Jones, R., & Breslauer, K. J., (1987) *Biochemistry 26*, 7150–7159.

Frank-Kamenetskii, M. D., & Vologodskii, A. V. (1984) *Nature (London) 307*, 481–482.

Freier, S. M., Kierzek, R., Jaeger, J. A., Sugimoto, N., Caruthers, M. H., Neilson, T., & Turner, D. H. (1986) *Proc. Natl. Acad. Sci. U.S.A. 83*, 9373–9377.

Gralla, J., & Crothers, D. M. (1973) *J. Mol. Biol. 73*, 497–511.

Hasnoot, C. A. G., de Hartog, J. H. J., de Rooij, J. F. M., van Boom, J. H., & Altona, C. (1980) *Nucleic Acids Res. 8*, 169–181.

Hasnoot, C. A. G., de Bruin, S. H., Berendsen, R. G., Janssen, H. G. J. M., Binnendijk, T. J. J., Hilbers, C. W., van der Marel, G. A., & van Boom, J. H. (1983) *J. Biomol. Struct. Dyn. 1*, 115–129.

Haasnoot, C. A. G., Hilbers, C. W., van der Marel, G. A., van Boom, J. H., Singh, U. C., Pattabiraman, N., & Kollman, P. A. (1986) *J. Biomol. Struct. Dyn. 3*, 843–857.

Hare, D. R., & Reid, B. R. (1986) *Biochemistry 25*, 5341–5350.

Hilbers, C. W., Hasnoot, C. A. G., de Bruin, S. H., Joorden, J. J., van der Marel, G. A., & van Boom, J. H. (1985) *Biochemie 67*, 685–695.

Hoiland, H. (1986) in *Thermodynamic Data for Biochemistry and Biotechnology* (Hinz, H. J., Ed.) Ch. 2, Springer-Verlag, Berlin, Heidelberg, New York, Toronto, and Tokyo.

Ikuta, S., Chattopadhyaya, R., Dickerson, R. E., & Kearns, D. R. (1986) *Biochemistry 25*, 4840–4849.

Lilley, D. M. J. (1980) *Proc. Natl. Acad. Sci. U.S.A. 77*, 6468–6472.

Lilley, D. M. J. (1981) *Nucleic Acids Res. 9*, 1271–1289.

Maniatis, T., Ptashne, M., Backman, K., Kleid, D., Flashman, S., Jeffrey, A., & Maurer, R. (1975) *Cell 5*, 109–113.

Manning, G. S. (1978) *Q. Rev. Biophys. 11*, 179–246.

Marky, L. A., & Breslauer, K. J. (1987) *Biopolymers 26*, 1601–1620.

Marky, L. A., & Kupke, K. J. (1989) *Biochemistry 28*, 9982–9988.

Marky, L. A., Kallenbach, N. R., McDonough, K. A., Seeman, N. C., & Breslauer, K. J. (1987) *Biopolymers 26*, 1621–1634.

Marky, L. A., Canuel, L., Jones, R. A., & Breslauer, K. J. (1981) *Biophys. Chem. 13*, 141–149.

Marky, L. A., Blumenfeld, K. S., Kozlowski, S., & Breslauer, K. J. (1983) *Biopolymers 22*, 1247–1257.

Muller, U. R., & Fitch, W. M. (1982) *Nature (London) 298*, 582–585.

Panayotatos, N., & Wells, R. D. (1981) *Nature (London) 289*, 466–470.

Paner, T. M., Amaratunga, M., Doktycz, M. J. & Benight, A. S. (1990) *Biopolymers 29*, 1715–1731.

Patel, D. J., Kozlowski, S. A., Ikuta, S., Itakura, K., Bhatt, R., & Hare, D. R. (1983) *Cold Spring Harbor Symp. Quant. Biol. 47*, 197–206.

Privalov, P. L., & Filimonov, V. V. (1978) *J. Mol. Biol. 122*, 447–464.

Record, M. T., Jr., Anderson, C. F., & Lohman, T. M. (1978) *Q. Rev. Biophys. 11*, 103–178.

Rosenberg, M., & Court, D. (1979) *Annu. Rev. Genet. 13*, 319–351.

Sarvazyan, A. P., & Kharakoz, D. P. (1981) *Instrum. Exp. Tech. 24*, 782–785.

Senior, M. M., Jones, R. A., & Breslauer, K. J. (1988) *Proc. Natl. Acad. Sci. U.S.A. 85*, 6242–6246.

Shestimirov, V. N., & Sarvazyan, A. P. (1986) *Bull Otkryt Isobret. (Russ.)*, 43.

Summers, M. F., Byrd, R. A., Gallo, K. A., Samson, C. J., Zon, G., & Egan, W. (1985) *Nucleic Acids Res. 13*, 6375–6393.

Uhlenbeck, O. C., Borer, P. N., Dengler, B., & Tinoco, I. (1973) *J. Mol. Biol. 73*, 483–496.

Wells, R. D., Goodman, T. C., Hillen, W., Horn, G. T., Klein, R. D., Larson, J. E., Muller, U. R., Neuendorf, S. K., Panayotatos, N., & Stirdivant, S. M. (1980) *Prog. Nucleic Acid Res. Mol. Biol. 25*, 167–267.

Wemmer, D. E., & Benight, A. S. (1985) *Nucleic Acids Res. 13*, 8611–8620.

Wemmer, D. E., Chou, S. H., Hare, D. R., & Reid, B. R. (1985) *Nucleic Acids Res. 13*, 3755–3772.

Williamson, J. R., & Boxer, S. G. (1989a) *Biochemistry 28*, 2819–2831.

Williamson, J. R., & Boxer, S. G. (1989b) *Biochemistry 28*, 2831–2836.

Wolk, S., Hardin, C. C., Germann, M. W., van de Sande, J. H., & Tinoco, I., Jr. (1988) *Biochemistry 27*, 6960–6967.

Xodo, L. E., Manzini, G., Quadrifoglio, F., van der Marel, G. A., & van Boom, J. H. (1986) *Nucleic Acids Res. 14*, 5389–5398.

Xodo, L. E., Manzini, G., Quadrifoglio, F,. van der Marel, G. A., & van Boom, J. H. (1988a) *Biochemistry 27*, 6321–6326.

Xodo, L. E., Manzini, G., Quadrifoglio, F., van der Marel,

G. A., & van Boom, J. H. (1988b) *Biochemistry 27*, 6327–6331.

Zolandz, D. (1986) B.S. Chemistry Honors Thesis, Douglass College, Rutgers University.

Formation of 8-Hydroxy(deoxy)guanosine and Generation of Strand Breaks at Guanine Residues in DNA by Singlet Oxygen[†]

Thomas P. A. Devasagayam,[‡] Steen Steenken,[§] Maik S. W. Obendorf,[‡] Wolfgang A. Schulz,[‡] and Helmut Sies[*,‡]

Institut für Physiologische Chemie I, Universität Düsseldorf, Moorenstrasse 5, D-4000 Düsseldorf, FRG, and Max-Planck-Institut für Strahlenchemie, Stiftstrasse 34-36, D-4330 Mülheim, FRG

Received November 19, 1990; Revised Manuscript Received February 14, 1991

ABSTRACT: Singlet molecular oxygen ($^1O_2$) was generated in aqueous solution (H_2O or D_2O) at 37 °C by the thermal dissociation of the endoperoxide of 3,3′-(1,4-naphthylidene) dipropionate ($NDPO_2$). Guanosine and deoxyguanosine quench $^1O_2$ with overall quenching rate constants of 6.2×10^6 M^{-1} s^{-1} and 5.2×10^6 M^{-1} s^{-1}, respectively. Reaction with $^1O_2$ results in the formation of 8-hydroxyguanosine (8-OH-Guo) and 8-hydroxydeoxyguanosine (8-OH-dGuo), respectively, with a yield of 1.5% at 1 mM substrate with an $NDPO_2$ concentration of 40 mM; a corresponding 8-hydroxy derivative is not formed from deoxyadenosine. In D_2O the yield of 8-OH-Guo is 1.5-fold that in H_2O. Sodium azide suppresses 8-OH-Guo and 8-OH-dGuo production. In contrast, the hydroxyl radical scavengers, *tert*-butanol, 2-propanol, or sodium formate, do not decrease the production of the 8-OH derivatives. The formation of 8-OH derivatives is significantly increased (2–5-fold) by thiols such as dithiothreitol, glutathione, cysteine, and cysteamine. With use of a plasmid containing a fragment of the mouse metallothionein I promoter (pMTP3′) and a novel end-labeling technique, the position of $^1O_2$-induced single-strand breaks in DNA was examined. Strand breaks occur selectively at dGuo; no major differences (hot spots) were observed between individual guanines.

Electronically excited molecular oxygen (singlet oxygen, $^1O_2$)[1] may be generated by photochemical reactions through transfer of excitation energy to ground-state oxygen ($^3O_2$) from a suitable excited triplet-state sensitizer (photoexcitation). It can also be produced in biological systems by dark reactions (chemiexcitation), e.g., in lipid peroxidation, and by enzyme reactions such as those catalysed by lactoperoxidase, lipoxygenase, and chloroperoxidase (Cadenas & Sies, 1984; Kanofsky, 1989). $^1O_2$ is produced during photooxidation of a variety of biological compounds and xenobiotics. Since $^1O_2$ is relatively long-lived, with half-times in the range of microseconds, considerable diffusion of singlet oxygen is possible with a radius estimated to be in the range of 100 Å (Schnuriger & Bourdon, 1968; Moan, 1990).

Singlet oxygen has been shown to be capable of inducing DNA damage and to be mutagenic (for review, see Piette (1990)). The guanine moiety has been observed to become hydroxylated at C8 on photolysis of oxygenated DNA solutions in the presence of the sensitizer methylene blue (Floyd et al., 1989). It was concluded that $^1O_2$ is the species responsible for this reaction, in agreement with the fact that $^1O_2$ reacts preferentially with free guanine nucleotides (Piette & Moore, 1982; Cadet et al., 1983; Kawanishi et al., 1986). Hence, it is of interest to ascertain whether $^1O_2$ is capable of forming 8-OH derivatives with guanosines and study possible factors influencing their formation. 8-Hydroxylation of guanine has also been identified as an important process in OH[·] radical induced damage to DNA (Floyd et al., 1986, 1988; Kasai et al., 1986; Aruoma et al., 1989). 8-OH-dGuo is a reaction product that can be easily measured and that has therefore been used as an indicator of oxidative DNA damage in vivo (Floyd et al., 1986; Kasai et al., 1986).

The $^1O_2$-induced damage to DNA also leads to strand breaks (Wefers et al., 1987; Di Mascio et al., 1989a, 1990). Decuyper-Debergh et al., (1987) have shown that $^1O_2$-induced mutagenicity results from single nucleotide substitutions occurring predominantly at the guanosine residues. However, the method is indirect since it involves measuring base substitutions after repair. Using a newly developed method that allows the detection of end-labeled nicked fragments on sequencing gels, we assign here the base position at which $^1O_2$-induced single-strand breaks occur in plasmid DNA and check the possibility of the occurrence of "hot spots".

Recent studies (Rougee et al., 1988; Kaiser et al., 1989; Devasagayam et al., 1991a) have shown that thiols and sulfur-containing amino acids quench $^1O_2$. Interestingly, if performed in the presence of DNA, this quenching is accompanied by a large increase in the number of strand breaks

[1] Abbreviations: $^1O_2$, singlet molecular oxygen; NDP, 3,3′-(1,4-naphthylidene) dipropionate; $NDPO_2$, endoperoxide of 3,3′-(1,4-naphthylidene) dipropionate; EDTA, ethylenediaminetetraacetic acid; DETAPAC, diethylenetriaminepentaacetic acid; OH[·], hydroxyl radical; 8-OH-Guo, 8-hydroxyguanosine; 8-OH-dGuo, 8-hydroxydeoxyguanosine; MTP, metallothionein promoter.